

## STRUCTURAL STUDY OF WATERPROOF THIN-LAYERS FOR THE MAGNETIC ALLOY CORE BY NEUTRON REFLECTIVITY

K. Akutsu<sup>†</sup>, M. Sahara, Comprehensive Research Organization for Science and Society (CROSS),  
Tokai, Japan.

T. Niizeki, S. Nagayama, Y. Hasegawa, ART KAGAKU Co., Ltd., Tokai, Japan.

M. Yoshii, J-PARC Center, KEK, Tokai, Japan.

A. Shimomura, Shimomurashikkiten Co., Ltd., Sabae, Japan.

### Abstract

The mechanism of the waterproof property of thin and thick SiO<sub>2</sub>(PHPS) layers was revealed by neutron reflectivity (NR) analysis. The NR analysis revealed that the thickness of the SiO<sub>2</sub>(PHPS) layers was 47 nm and 154 nm, respectively. In addition, the penetration depth of water into the thin and thick SiO<sub>2</sub>(PHPS) layers were estimated to be 44 nm and 5 nm, respectively. Namely water penetration depth increased with decreasing the thickness of the SiO<sub>2</sub>(PHPS) layer. These results suggest that the thick SiO<sub>2</sub>(PHPS) layer is more protective against water than the thin SiO<sub>2</sub>(PHPS) thin layer.

### INTRODUCTION

Silicon based ceramics such as perhydropolysilazane (PHPS) derived ceramics have been studied as coating materials to protect certain metallic components and other water sensitive materials [1]. PHPS is a useful material for the protection of metallic materials in corrosive environments. This is due to the fact that PHPS can be easily and simply used to synthesize high-quality SiO<sub>2</sub> layers on metallic materials through hydrolysis or oxidation of PHPS [1]. We have used the PHPS/xylene system to synthesize a SiO<sub>2</sub>-waterproof layer, denoted as SiO<sub>2</sub>(PHPS), for use in the magnetic alloy core of the accelerator ring in the Japan Proton Accelerator Research Complex (J-PARC), Tokai, Japan. The structure of the SiO<sub>2</sub>(PHPS) thin layer was studied by neutron reflectivity (NR), Fourier-transform infrared spectroscopy (FT-IR), and spectroscopic ellipsometry (SE) analysis [2, 3]. As a result, detailed SiO<sub>2</sub>(PHPS) thin layer structures and their cracking mechanism were elucidated. However, the water penetration behaviour of the SiO<sub>2</sub>(PHPS) thin layer have not yet been investigated in detail.

To obtain a thorough understanding of their waterproof properties, water penetration behaviour into the SiO<sub>2</sub>(PHPS) thin layer was studied using the NR analysis methods. Since the density of the SiO<sub>2</sub>(PHPS) layer increase with increasing the thickness of the layer, we prepared both thin (~70 nm) and thick (~180 nm) of SiO<sub>2</sub>(PHPS) layer samples to investigate the effect of the thickness on the water penetration behaviour of them. Because the density of the thick SiO<sub>2</sub>(PHPS) sample is higher than that of the thin sample, it is predicted that the water penetration rate of the thick SiO<sub>2</sub>(PHPS) sample is lower than that of the thin one. In this paper, we report the results of the NR analysis and discuss the waterproof behaviour and mechanism of these samples.

### EXPERIMENTAL

#### Sample Preparation

The Si wafers (diameter = 5.08 cm, thickness = 0.3 mm) were supplied by SEMITEC Co., Ltd., Tokyo, Japan. The PHPS polymer was supplied by AZ Electronic Materials Co., Ltd., Tokyo, Japan. The thin and thick SiO<sub>2</sub>(PHPS) layer samples were prepared by spin coating 3.3 % and 10.0 % of PHPS polymer/xylene solution onto Si substrates at a speed of 6000 rpm, respectively, using a spin-coater (MS-A150, Mikasa Co., Ltd., Tokyo, Japan). These samples were then cured at 60 °C for 1 h and allowed to stand for 48 h at room temperature. These samples were stored in deuterium oxide (D<sub>2</sub>O) solution for 3 days, and then they were dried in a dry nitrogen gas box for 1 h before the NR experiment to remove the non-adsorbed water molecules. These samples were stored in the dry nitrogen gas box at room temperature before starting the NR experiments.

#### Neutron Reflectivity Measurements

The NR measurements were performed using a BL17 SHARAKU polarized neutron reflectometer installed at the Materials and Life Science Experimental Facility (MLF) in J-PARC [4]. The incident beam power of the proton accelerator was 150 kW for all the measurements. Pulsed neutron beams were generated in mercury target at 25 Hz, and the NR data were measured using the time-of-flight (TOF) technique [3]. The wavelength ( $\lambda$ ) range of the incident neutron beam was tuned to approximately  $\lambda = 1.1 - 8.8 \text{ \AA}$  by a disk chopper. The incident angle was varied from 0.3° to 1.2°, and the exposure times for measurements at incident angles of 0.3° and 1.2° were 0.5 and 1 h, respectively. The covered  $Q_z$  range was  $Q_z = 0.008 - 0.20 \text{ \AA}^{-1}$ , where  $Q_z = (4\pi/\lambda)\sin\theta$  ( $\theta$  represents the incident angle). A 25 mm beam footprint was maintained on the sample surface by using six different kinds of incident slits [4]. All the measurements were performed at room temperature. The data reduction, normalization, and subtraction were performed using a program installed in BL17 SHARAKU. The Motofit program [5] was used to fit the NR profiles with a least-squares approach to minimize the deviation of the fit. The thickness, scattering length density (SLD,  $\rho$ ), and Gaussian roughness were also evaluated by using the Motofit program.

## RESULTS AND DISCUSSION

### Neutron Reflectivity Analysis

To investigate the effect of water penetration into the thin and thick SiO<sub>2</sub>(PHPS) layer samples, the structure of the samples, which were stored in D<sub>2</sub>O for 3 days, were studied by the NR analysis method in detail.

The air-solid reflectivity measurements for the dry and wet SiO<sub>2</sub>(PHPS) thin layer samples are shown in Figure 1. The NR profiles of the samples were analysed using the Motofit reflectometry package, and the calculated theoretical reflectivity profiles are also shown in Figure 1. The circles represent the observed NR profiles, while the solid lines represent the calculated NR profiles determined from the structural models. The NR profiles of the wet thin SiO<sub>2</sub>(PHPS) layer sample were drastically different from those of the dry sample. In addition, the peaks of Kiessig fringes become clear. It is because the difference of the SLD between Si substrate and SiO<sub>2</sub>(PHPS) layer becomes larger. These changes imply that water molecules were penetrated deeper into the SiO<sub>2</sub>(PHPS) layer. In addition, a naturally oxidized thin SiO<sub>2</sub> layer formed between the SiO<sub>2</sub>(PHPS) layer and the Si substrate, a three-layer model, SiO<sub>2</sub>(PHPS) wet /SiO<sub>2</sub>(PHPS) dry/ SiO<sub>2</sub>(oxidized)/Si, was applied to fit the obtained NR profiles. As shown in Figure 1, the theoretical reflectivity profiles reproduced the experimental NR profiles in the all  $Q_z$ -range. Table 1 shows the structural parameters obtained from this analysis. The thickness ( $t$ ) and SLD ( $\rho$ ) values of the dry thin SiO<sub>2</sub>(PHPS) layer sample were estimated to be 472 Å and  $2.30 (\times 10^{-6} \text{ \AA}^{-2})$  for SiO<sub>2</sub>(PHPS) layer and 7.3 Å and  $3.47 (\times 10^{-6} \text{ \AA}^{-2})$  for SiO<sub>2</sub>(oxidized) layer, respectively. On the other hand, the  $t$  and  $\rho$  values of the wet thin SiO<sub>2</sub>(PHPS) layer sample were estimated to be 436 Å and  $2.73 (\times 10^{-6} \text{ \AA}^{-2})$  for SiO<sub>2</sub>(PHPS) wet layer, 26.1 Å and  $2.30 (\times 10^{-6} \text{ \AA}^{-2})$  for SiO<sub>2</sub>(PHPS) dry layer, and 9.6 Å and  $3.47 (\times 10^{-6} \text{ \AA}^{-2})$  for SiO<sub>2</sub>(oxidized) layer, respectively. Because higher SLD values indicate penetration of D<sub>2</sub>O ( $\rho$  value =  $6.34 (\times 10^{-6} \text{ \AA}^{-2})$ ) molecules into the layers, the obtained high  $\rho$  value (2.73) clearly indicate that a large amount of D<sub>2</sub>O is present into the SiO<sub>2</sub>(PHPS) layer. Depth profile of the thin SiO<sub>2</sub>(PHPS) layer samples drawn in Figure 1 also indicates that the water molecules were penetrated into the surface of the Si substrate.

The air-solid reflectivity measurements for the dry and wet SiO<sub>2</sub>(PHPS) thick layer samples are shown in Figure 2. The NR profiles of the samples were analysed using the Motofit reflectometry package, and the calculated theoretical reflectivity profiles are also shown in Figure 2. The circles represent the observed NR profiles, while the solid lines represent the calculated NR profiles determined from the structural models. There was a little difference between the NR profiles of the dry sample and that of the wet one. It implied that water molecules were penetrated only into the surface of the SiO<sub>2</sub>(PHPS) layer. Therefore, a three-layer model, SiO<sub>2</sub>(PHPS) wet /SiO<sub>2</sub>(PHPS) dry/ SiO<sub>2</sub>(oxidized)/Si, was applied to fit the obtained NR profiles. As shown in Figure 2, the theoretical reflectivity profiles reproduced the experimental NR profiles in the all  $Q_z$ -range.

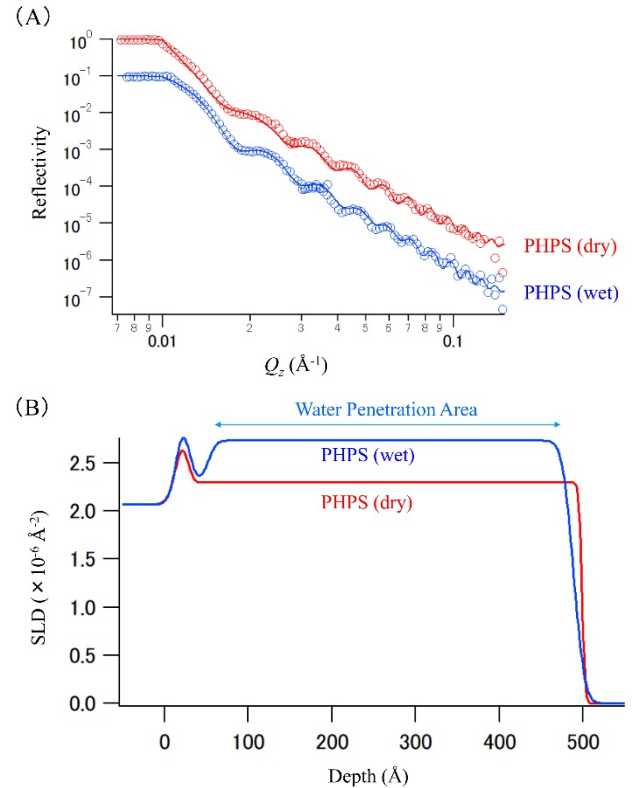


Figure 1: (A) NR profiles of the dry and wet SiO<sub>2</sub>(PHPS) thin layer samples. The circles represent the experimental data, and the solid lines represent the best-fit calculated NR profiles. (B) Depth profiles of the dry and wet SiO<sub>2</sub>(PHPS) thin layer samples calculated by obtained structural parameters.

Table 1: Best-fit Parameters for the Reflectivity Model Data Shown in Figure 1.

|  |  | dry sample | wet sample |
|--|--|------------|------------|
| SiO <sub>2</sub> (PHPS)<br>(wet layer) | $t$ (Å)                                      | -          | 436        |
|  | $\rho$ ( $\times 10^{-6} \text{ \AA}^{-2}$ ) | -          | 2.73       |
|  | $\sigma$ (Å)                                 | -          | 10.5       |
| SiO <sub>2</sub> (PHPS)<br>(dry layer) | $t$ (Å)                                      | 472        | 26.1       |
|  | $\rho$ ( $\times 10^{-6} \text{ \AA}^{-2}$ ) | 2.30       | 2.30       |
|  | $\sigma$ (Å)                                 | 3.2        | 7.7        |
| SiO <sub>2</sub><br>(oxidized)         | $t$ (Å)                                      | 7.3        | 9.5        |
|  | $\rho$ ( $\times 10^{-6} \text{ \AA}^{-2}$ ) | 3.47       | 3.47       |
|  | $\sigma$ (Å)                                 | 6.8        | 8.0        |
| Si substrate                           | $\rho$ ( $\times 10^{-6} \text{ \AA}^{-2}$ ) | 2.07       | 2.07       |
|  | $\sigma$ (Å)                                 | 9.7        | 8.2        |

$t$ : thickness,  $\rho$ : SLD,  $\sigma$ : roughness of the surface or interface.

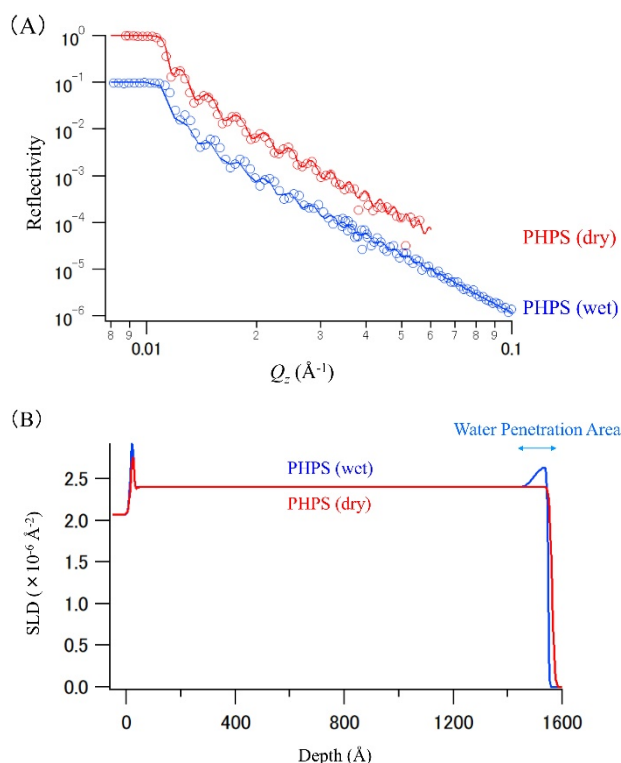


Figure 2: (A) NR profiles of the dry and wet SiO<sub>2</sub>(PHPS) thick layer samples. The circles represent the experimental data, and the solid lines represent the best-fit calculated NR profiles. (B) Depth profiles of the dry and wet SiO<sub>2</sub>(PHPS) thick layer samples calculated by obtained structural parameters.

Table 2: Best-fit Parameters for the Reflectivity Model Data Shown in Figure 2.

|  |   | dry sample | wet sample |
|--|---|------------|------------|
| SiO <sub>2</sub> (PHPS)<br>(wet layer) | $t$ (Å)                                     | -          | 52.2       |
|  | $\rho$ ( $\times 10^{-6}$ Å <sup>-2</sup> ) | -          | 2.64       |
|  | $\sigma$ (Å)                                | -          | 3.5        |
| SiO <sub>2</sub> (PHPS)<br>(dry layer) | $t$ (Å)                                     | 1535       | 1470       |
|  | $\rho$ ( $\times 10^{-6}$ Å <sup>-2</sup> ) | 2.40       | 2.40       |
|  | $\sigma$ (Å)                                | 7.8        | 21.4       |
| SiO <sub>2</sub><br>(oxidized)         | $t$ (Å)                                     | 7.0        | 8.4        |
|  | $\rho$ ( $\times 10^{-6}$ Å <sup>-2</sup> ) | 3.47       | 3.47       |
|  | $\sigma$ (Å)                                | 4.5        | 4.0        |
| Si substrate                           | $\rho$ ( $\times 10^{-6}$ Å <sup>-2</sup> ) | 2.07       | 2.07       |
|  | $\sigma$ (Å)                                | 8.6        | 6.66       |

$t$ : thickness,  $\rho$ : SLD,  $\sigma$ : roughness of the surface or interface.

Table 2 shows the structural parameters obtained from this analysis. The thickness ( $t$ ) and SLD ( $\rho$ ) values of the dry thin SiO<sub>2</sub>(PHPS) layer sample were estimated to be 1535 Å and  $2.40 (\times 10^{-6} \text{ Å}^{-2})$  for SiO<sub>2</sub>(PHPS) layer and 7.0 Å and  $3.47 (\times 10^{-6} \text{ Å}^{-2})$  for SiO<sub>2</sub>(oxidized) layer, respectively. On the other hand, the  $t$  and  $\rho$  values of the wet thick SiO<sub>2</sub>(PHPS) layer sample were estimated to be 52 Å and  $2.64 (\times 10^{-6} \text{ Å}^{-2})$  for SiO<sub>2</sub>(PHPS) wet layer, 1470 Å and  $2.40 (\times 10^{-6} \text{ Å}^{-2})$  for SiO<sub>2</sub>(PHPS) dry layer, and 8.4 Å and  $3.47 (\times 10^{-6} \text{ Å}^{-2})$  for SiO<sub>2</sub>(oxidized) layer, respectively. As mentioned above, the obtained high  $\rho$  value (2.62) clearly indicate that D<sub>2</sub>O is present into the SiO<sub>2</sub>(PHPS) layer. Depth profile of the thin SiO<sub>2</sub>(PHPS) layer samples drawn in Figure 2 also indicates that the water molecules were penetrated into the surface of the SiO<sub>2</sub>(PHPS) layer. These results suggested that the water protection ability of SiO<sub>2</sub>(PHPS) coatings increase with increasing the thickness of the protection layer, and only 5 nm water penetration was observed in the 140 nm SiO<sub>2</sub>(PHPS) coating sample.

## CONCLUSION

In this study, the structure of the SiO<sub>2</sub>-waterproof layer, SiO<sub>2</sub>(PHPS), was investigated in detail by the NR analysis method. The analyses revealed that the penetration depth of water into the thin and thick (PHPS) layers was estimated to be 436 Å and 52 Å, respectively. Under service conditions, the magnetic alloy core is covered with 1  $\mu\text{m}$  of SiO<sub>2</sub>(PHPS) waterproofing layer. This indicates that water penetration can be sufficiently prevented in the service condition. Therefore, it can be suggested that the thick SiO<sub>2</sub>(PHPS) layer has a great potential for utilization as an effective waterproof SiO<sub>2</sub> coating material.

## ACKNOWLEDGEMENT

We thank Dr. K. Soyama (JAEA), Dr. H. Aoki (JAEA) for their supports with regard to the NR experiments. The NR experiments were conducted at the BL17 SHARAKU of the Materials and Life Science Experimental Facility (MLF) in J-PARC (Proposal No.2016I0017). All sample preparation experiments were conducted at the User Experiment Preparation Lab III provided by CROSS.

## REFERENCES

- [1] K. Sato *et al.*, J. Ceram. Soc. Jpn., 109, 440–446 (2001).
- [2] K. Akutsu *et al.*, J. Ceram. Soc. Jpn., 124, 172–176 (2016).
- [3] T. Niizeki *et al.*, Coatings., 6, 64 (2016).
- [4] M. Takeda *et al.*, Chinese J. Phys., 50, 161–170 (2012).
- [5] A. Nelson *et al.*, Langmuir, 22, 453–458 (2006).